

The Electro-Anatomical Pathway for Normal and Abnormal ECGs in COVID Patients

Peter M van Dam^{1,3}, Machteld Boonstra¹, Rob Roudijk¹, Marijke PM Linschoten¹, Emanuela T Locati², Peter Loh¹

¹University Medical Center Utrecht, The Netherlands, ²IRCCS Policlinico San Donato, Milano, Italy,

³ECG Excellence BV, Nieuwerbrug aan den Rijn, Netherlands

Abstract

Patients with COVID-19 frequently have non-typical ECG changes in the QRS and T-wave morphology. The novel CineECG uses using the mean temporal spatial isochrones (mTSI) to relate the activation and recovery pathway to the cardiac anatomy. The aim of this feasibility study is to use the novel CineECG to separate normal from abnormal ECGs.

The ECGs of 100 normal controls were used to obtain the normal mTSI paths values for the QRS, ST segment and T-wave. These normal CineECG values were used to classify the COVID-19 ECGs as either as normal or abnormal of 107 patients being treated for COVID-19 in the University Medical Center Utrecht.

The CineECG was able to classify 98% of the normal ECG correctly and 94% of the abnormal ECG in comparison to expert ECG classifications.

The ability of the CineECG to relate the ECG to the cardiac anatomy supports the detection of abnormal ECGs. The CineECG might be a novel ECG screening tool to detect potential cardiac involvement of the COVID-19 disease for non-ECG experts.

1. Introduction

COVID-19 is often associated with cardiovascular complications thereby further increasing the yet huge burden on the health care system [1,2]. The combination of COVID-19 and cardiovascular disease makes that the patient is at high-risk for complications during the treatment. Early recognition of cardiac dysfunction amongst COVID-19 patients is therefore of great importance to optimize for personalized and cardiac treatment. The detection of potential cardiac problems currently requires the involvement of the specialized cardiologist. The ECG of COVID-19 patients with cardiovascular complications show tachycardias, conduction disorders and atypical T-wave morphology changes. The detection of cardiac complications in the

COVID-19 population might be improved by the CineECG technology, using the standard 12 lead ECG, relates the ECG waveforms directly to the cardiac anatomy.

This study presents the preliminary results on the detection of deviating ECG waveforms using the CineECG. To determine the normal values for the CineECG, we used 100 normal subjects from the PTB-XL database [3]. The COVID-19 ECGs were obtained from the international Capacity-COVID patient registry. The normal range of specific CineECG parameters were used to classify an ECG from a COVID-19 patient as normal or abnormal.

Aim of the study

The aim of the study was to reduce the burden on cardiac testing and detect cardiac complications during ICU admission by using CineECG derived from the standard 12 lead ECG.

2. Methods

2.1. Patient Selection

We selected 121 COVID-19 patients from the Capacity-COVID database(www.capacity-covid.eu). Routine 12-lead ECGs (GE Healthcare, MAC5500) were obtained according to standard clinical care during COVID-19 related hospital admissions at the UMC Utrecht. Subjects were retrospectively included in the Capacity-COVID registry and could be excluded via an opt-out procedure. Of all included subjects, raw ECG recordings were exported and used for analysis. The ECGs were re-examined and classified as normal or abnormal by author RR. ECGs classified as both abnormal and not in sinus rhythm were excluded for analysis as well as ECGs where the secondary evaluation did not coincide with the database classification. After exclusion 80 patients were included in the study, with 107 ECGs in total. These 107 ECGs, either normal or abnormal, were further divided in

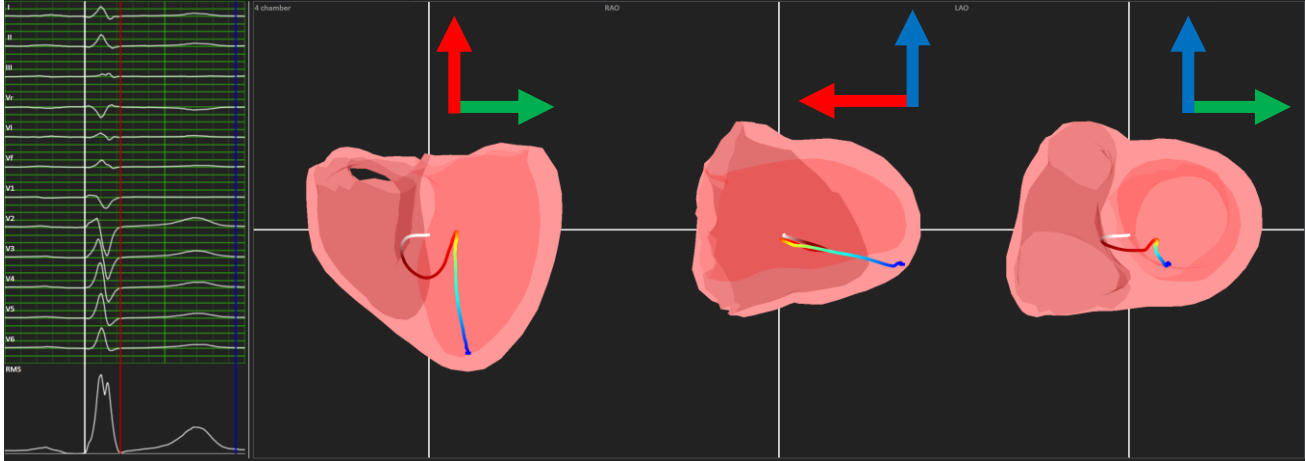


Figure 1: An example of the mTSI of a normal subject from the PTB-XL database. In the panel the 12 lead ECG is shown left with the root mean square signals in the bottom left corner. The QRS onset is indicated by a white line, the QRS end with a red line and the end of the T wave with a blue line. These colors can also be found in the mTSI shown as a colored line through the ventricles. The ventricles are shown in standard X-ray views: the 4 chamber view (left panel), Right Anterior Oblique (RAO) view (middle panel) and the Left Anterior Oblique view (LAO). The 3 heart axis are shown as red, blue and green arrows. The initial mTSI (white) travels clearly trans-septal (4 chamber view) and moves then to the left chamber (red part), as more ventricular mass is activated on the left. During the ST segment (yellow/green line) and the T-wave (blue line) the mTSI moves towards the left apex of the heart.

two patient groups based on information from the capacity database: a group with known cardiac history and one without prior to the Covid-19 disease. Of the included patients, 23 patients were known with a cardiac history of conduction disorders or an arrhythmia, 9 patients with heart failure, 25 with coronary artery disease, 7 with a valvular disease, and 7 patients remained unclassified. For 10 patients more than one classification was used.

The data for the normal values was a selection of 100 ECGs labeled as normal from the PTB-XL database [1]. The average age for normal group was 48 ± 17 years with 52% females. For the 80 Covid-19 patients the average age was 66 ± 13 years with 34% females.

2.2. The CineECG

The CineECG computes the mean temporal-spatial isochrones (mTSI), representing the mean activation and recovery pathway of the heart. In this study we will focus on the ventricular activation and recovery, where mTSI was related directly to the ventricular anatomy. Therefore, the CineECG not only needs the 12 lead ECG, but also a model of the heart and the locations of the electrodes on the chest, building the sensor (electrodes) source (ventricles) relationship. The mTSI is computed from the 12 lead ECG in 2 steps [4]. In the first step a vector cardiogram (VCG) is computed using the known torso and limb electrode positions relative to the heart. The VCG thus gives the direction of activation or recovery at any time instant of the ECG. In step 2 of the CineECG algorithm this direction is used to move the mTSI with a predefined velocity. The activation path direction is based on the VCG direction per time sample, using a propagation

velocity of 0.7 m/s through the myocardium for the QRS and 0.25 for the -Wave [5].

The first point of the mTSI should be chosen close to the initial activation of the heart, which is for normal sinus rhythm on the left septal wall. For this reason, the QRS initiation site of the mTSI is chosen to the septal location closest to the center of ventricular mass.

At last, the computed mTSI was directly related and visualized into the 3D heart space, using three standard 2D X-ray views (Figure 1). For the current study the heart and torso model of a 58-year-old male was used [5].

2.3. ECG and mTSI definitions

The definition of a normal and abnormal ECG is based on a number of ECG and mTSI definition. In a previous study we used these mTSI parameters to classify an ECG beat as incomplete and complete right bundle branch block ((I)RBBB) [5]. Additional parameters used in this study:

QRST definitions: For each beat the QRS duration is determined, as well as the ST ratio. The ST ratio is defined as the averaged amplitude of ST segment (up to 60 ms after the QRS end) of the root mean square signal divided by the peak T wave amplitude of the same signal (see Figure 1).

Trans-cardiac ratio (TCR): The trans-cardiac ratio is defined as the 3D-distance between the starting and the ending points of the mTSI during activation, coincident with the QRS onset to the QRS offset. As this measure is influenced by the size of the heart, it was weighted by the size of the heart model, resulting as a relative number.

mTSI direction: The direction of the mTSI, representing the direction of electrical activity, is related to the heart axis. In this study the *terminal ST direction* ($QRS_{end} - T$

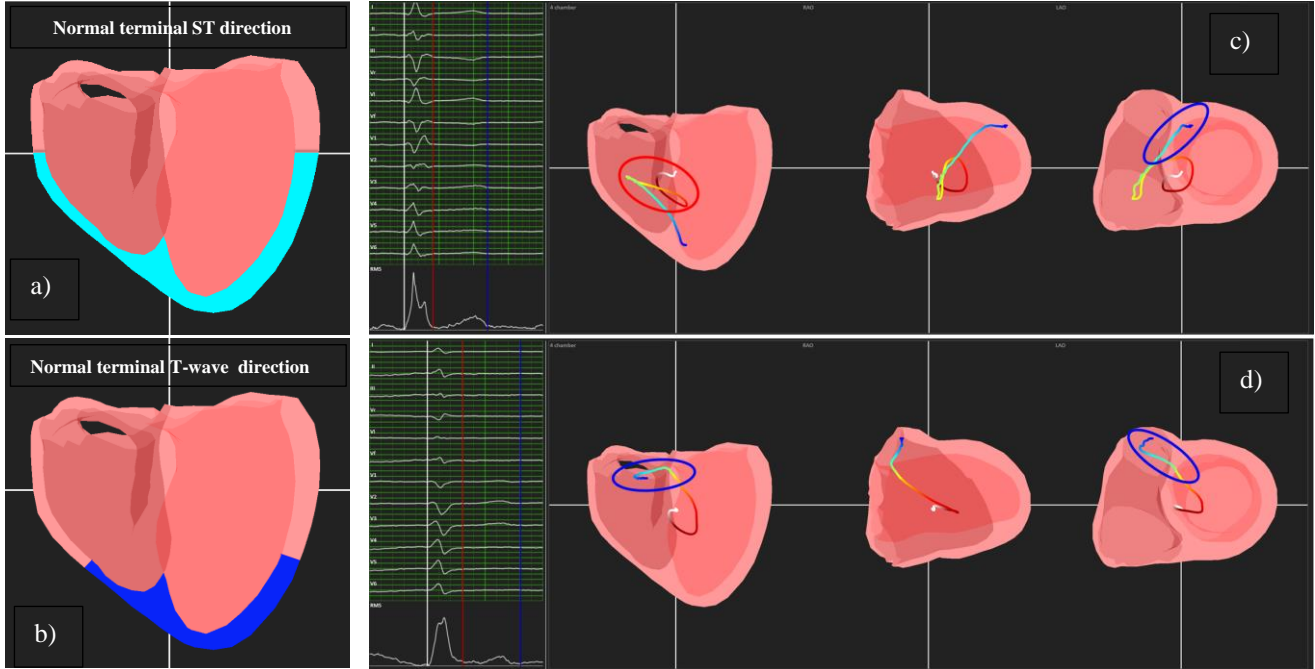


Figure 2: The normal terminal ST (panel a) and terminal T-wave (panel b) directions of the mTSTI. When the mTSTI terminal directions of a COVID patient was found outside this direction, the ECG beat was classified as abnormal. panel c) visualizes the mTSTI pathway from a patient without cardiac history. Delayed QRS activation can be observed towards the right chamber with a large trans-cardiac ratio of more than 37%, terminal ST and T-wave direction classified as normal. The patient in panel d) shows a more compact mTSTI QRS pathway classified as normal, but the terminal ST- and T-wave directions are now far from normal, consequently the ECG beat was classified as abnormal. Deviating part of the mTSTI pathway are encircled in red (QRS related) and in blue (T-wave related). In panels c) and d) the 12 lead ECG is shown. See figure 1 for heart planes description.

wave_{peak}) and the terminal T wave direction (T-wave_{peak-end}) were computed. For every normal control from the PTB-XL database the mTSTI and ECG parameters were computed for up to 8 ECG beats with a similar morphology. The range of each of these normal parameter values determined the normal range used in the analysis.

3. Results

The ranges of the ECG and mTSTI parameters from the normal controls (PTB-XL [3]) were used to classify the QRST wave morphology as normal or abnormal, being:

- QRS duration: ≤ 104 ms
- Trans-cardiac ratio $< 37\%$
- ST ratio: ≤ 0.33 , i.e. peak T-wave $> 3 \cdot$ ST amplitude
- Terminal ST direction toward the lower apical half of the ventricles, see Figure 2a for the indicated area in cyan.
- Terminal T-wave direction towards the septal apex, see Figure 2b for the indicated apical area in blue.

When any of the selected parameter values was outside the normal range listed above, the ECG was classified as abnormal. The CineECG classification of either normal or abnormal was compared to the classification from the Capacity-COVID database. The results and the CineECG parameters used to classify the ECG are listed in Table 1. One out of 43 COVID-19 normal ECGs was classified as

abnormal, and for 4 ECG of 64 abnormal ECG the classification was normal. Examples of abnormal mTSTI paths in Figure 2.

Table 1 CineECG classification of 107 ECG's from COVID-19 patients based on the ventricular waveform of the ECG beats. All parameter values given in %. Some of the classifications overlap, e.g. the ST direction can be normal and T-wave direction abnormal, or both can be abnormal. Therefor only the total percentage per ECG groups add up to 100%. TCR = trans-cardiac ratio.

ECG class	Classification Parameter	Normal ECG		Abnormal ECG	
		No History	Cardiac History	No History	Cardiac History
Normal	QRS (≤ 104 ms)	100	100	41	32
	Terminal ST direction	100	100	64	76
	Terminal T-wave direction	97	100	64	32
	Total	97	100	5	8
Ab - normal	(I)RBBB	0	0	36	20
	QRS (> 104 ms)	0	0	51	60
	TCR ($> 37\%$)	0	0	21	36
	ST ratio (> 0.33)	0	0	46	32
	Terminal ST direction	0	0	31	20
	Terminal T-wave direction	3	0	33	80
	Total	3	0	95	92
Total number ECGs		34	9	39	25

4. Discussion

This feasibility study shows that the CineECG might be able to classify ECG waveforms to normal or abnormal, a much needed feature required in the critical unit to identify COVID-19 patients at cardiovascular risk. The CineECG classification was derived from 5 parameters, QRS duration, ST ratio, trans-cardiac ratio, and the terminal ST and T-wave direction. The last 3 CineECG parameters are novel as they classify the activation and recovery pathway (mTSI) in relation to the cardiac anatomy, which prove to be able to identify normal from abnormal QRS complex and T-waves (Table 1, Figure 2).

In a previous study we have shown that the mTSI of the QRS and early ST segment can be used to identify Brugada patients due to the terminal QRS direction towards the RVOT. The initial results of study show that this can also be used for the recovery of the heart, the T-wave. The T-wave direction of the normals is remarkably consistent in that it follows more or less the septum of the generic heart model, even when most probably the normal subjects must have had a different body build and thus a different heart orientation. A part of the variation of the T-wave direction in the normal population is therefore also attributed to this variation in heart orientation. Further study, using patient specific models of the heart is required to quantify this variation, and to confirm that the normal mTSI direction follows the septum.

The terminal ST direction is less specific than the terminal T-wave direction. As indicated in the Brugada study [5], the ST segment can be used to detect and classify conduction disorders. In this study only the trans-cardiac ratio in combination with the QRS duration (> 104 ms) was used to detect evolving conduction disorders in the COVID database. The assumption was that no conduction disorders were present in the normal controls all with a QRS duration of less than 104 ms.

4.2. Limitations

The used planes to project the mTSI are dependent on the patient specific orientation and position of the heart in the thorax. For this study, we used a standard heart and thorax model, which influences the results of this study. Moreover, the number of COVID-19 patients included in the study was limited and the background of these COVID-19 patients was not always known. Further studies are required therefore.

Also, where CineECG takes patient-specific electrode positioning into account, seriously misplaced 12-lead ECG electrodes (more than 2-4 cm) might cause misinterpreted mTSI measurements.

5. Conclusion

The CineECG is not only able to classify the QRS waveform as normal or abnormal, but also the ST segment and the T-wave. The establishment of the direct anatomical relation in 3D of the mTSI to the cardiac anatomy might enable the early warning of developing ischemia and myocarditis frequently occurring in COVID-19 patients. The CineECG might thus be a useful tool to screen COVID-19 patients without the immediate need of the expert cardiologist.

Acknowledgements

This study was funded by Health Holland, project COCVD grant number LSHM 20034 and Dutch Heart Foundation, grants QRS-Vision and eDetect.

Peter van Dam is the owner of ECG Excellence BV and Peacs BV (the Netherlands).

We would like to thank Prof. Dr. F.W. Asselbergs UMC Utrecht) for providing the data from the CAPACITY-COVID collaborative. Other collaborators are:

Admiraal de Ruyter Hospital, Goes, the Netherlands - van Kesteren HAM | Albert Schweitzer Hospital, Dordrecht, the Netherlands - van de Watering DJ | Amphibia Hospital, Breda, The Netherlands - Schaap J, Alings AMW | Amstelland Hospital, Amstelveen, the Netherlands - Koning AMH | Amsterdam University Medical Center, Amsterdam, the Netherlands - Pinto Y, Tjong FVY | Antonius Hospital, Sneek, the Netherlands - de Vries JK | A.O.U. San Luigi Gonzaga, Orbassano, Italy - Montagna LM, Bianco MB, Mazzilli SGM | Barts Health NHS Trust, London, United Kingdom - Saxena M | Beatrix Hospital, Gorinchem, the Netherlands - Westendorp PHM | Bernhoven Hospital, Uden, the Netherlands - van de Wal RMA | Bravis Hospital, Roosendaal, the Netherlands - Dorman HGR, van Boxem AJM | Catharina Hospital, Eindhoven, the Netherlands - Tio RA | CHU UCL Namur - Site Godinne, Yvoir, Belgium - Gabriel LG | Clinic University Hospital, INCLIVA Health Research Institute, Valencia, Spain - Redón J, Forner MJ | Deventer Hospital, Deventer, the Netherlands - Badings EA | Diaconessenhuis, Utrecht, the Netherlands - van Ofwegen-Hanekamp CEE | Dijklander Hospital, Hoorn, the Netherlands - Wierda E | Dutch Network for Cardiovascular Research, Utrecht, the Netherlands - Schut A | Elisabeth-Tweesteden Hospital, Tilburg, the Netherlands - Monraats PS | EMMS Hospital, Nazareth, Israel - Hellou EH | Erasmus Medical Center, Rotterdam, the Netherlands - den Uil CA, Jewbali LS | Fransiscus Gasthuis, Rotterdam, the Netherlands - Nierop PR | Fransiscus Vlietland, Schiedam, the Netherlands - van der Linden MMJM | Gelre Hospital, Zutphen, the Netherlands - Al Windy NY | Gelre Hospital, Apeldoorn, the Netherlands - Groenemeijer BE | Groene Hart Hospital, Gouda, the Netherlands - van Hessen MWJ | Haaglanden

Medical Center, the Hague, the Netherlands – van der Heijden DJ | Hospital do Espírito Santo, Évora, Portugal – Ribeiro MIA | Hospital Prof. Doutor Fernando Fonseca, Amadora, Portugal – Ferreira JB | Hospital Universitario Virgen de las Nieves, Granada, Spain - Macías-Ruiz RMR | Ikazia Hospital, Rotterdam, the Netherlands – Emans ME | I.M. Sechenov First Moscow State Medical University, Moscow, Russia – Kopylov PY, Blagova OV | Isala Hospital, Zwolle, the Netherlands – Hermanides RS | Jeroen Bosch Hospital, s-Hertogenbosch, the Netherlands - Haerkens-Arends HE | Jessa Hospital, Hasselt, Belgium - Timmermans P Jr, Messiaen P | Julius Center for Health Sciences and Primary Care, Utrecht, the Netherlands – van Smeden M | King Fahd Hospital of the University, Imam Abdulrahman Bin Faisal University, Kobar, Saudi Arabia - Al-Ali AK, Alshehri AM, Alnafie AN, Alshahrani M, Almubarak YA, Al-Muhanna FA, Al-Rubaish AM | Lange Land Hospital, Zoetermeer, the Netherlands – van der Meer, P | Leeds Teaching Hospital NHS Trust, Leeds, United Kingdom – Kearney M | Medical Center Leeuwarden, Leeuwarden, the Netherlands – van den Brink FS | Leiden University Medical Center, Leiden, the Netherlands – Siebelink HJ | Maasstad Hospital, Rotterdam, the Netherlands – Smits PC | Maastricht University Medical Center, Maastricht, the Netherlands – Heymans SRB | Martini Hospital, Groningen, the Netherlands – Tieleman RG, Reidinga AC | Meander Medical Center, Amersfoort, the Netherlands – Mosterd A | Medisch Spectrum Twente, Enschede, the Netherlands – Meijjs MFL, Delsing CE, van Veen HPAA | Netherlands Heart Institute, Utrecht, the Netherlands – Hermans – van Ast W, Iperen EPA | Northumbria Healthcare NHS Foundation Trust, Newcastle upon Tyne, United Kingdom - Aujayeb A | One Day Surgery Hospital, Cairo, Egypt – Salah R | Rijnstate Hospital, Arnhem, the Netherlands – Seelig J | Rode Kruis Hospital, Beverwijk, the Netherlands – Westendorp ICD, Veldhuis LI | Royal Devon and Exeter NHS Foundation Trust, Exeter, United Kingdom – Shore AC | Royal Free Hospital NHS Trust, London, United Kingdom – Captur G | Salford Royal NHS Foundation Trust, Salford, United Kingdom – Dark P | Saxenburgh Medical Center, Hardenberg, the Netherlands – Drost JT | Slingeland Hospital, Doetinchem, the Netherlands – Schellings DAAM | Southern Health and Social Care Trust, Portadown, United Kingdom - Moriarty A | Spaarne Gasthuis, Haarlem, the Netherlands – Kuijper AFM | SSR Val Rosay, Saint Didier au Mont d'Or, France – Charlotte NC | St. Antonius Hospital, Nieuwegein, the Netherlands – ten Berg JM | St. Jansdal Hospital, Harderwijk, the Netherlands – van der Zee PM | Tehran Heart Center, Tehran, Iran - Shafiee A, Hedayat B, Saneei E, Poorhosseini H | The Newcastle Upon Tyne NHS Foundation Trust, Newcastle Upon Tyne, United Kingdom – Zaman A | The Antwerp University Hospital, Antwerp, Belgium - van Craenenbroeck EM, van Ierssel S, Kwakkel-van Erp H | Treant Zorggroep, Emmen, the

Netherlands – Anthonio RL | University College London Hospitals NHS Foundation Trust, London, United Kingdom – Williams B, Patel RS, Bell R | University Hospitals Bristol NHS Foundation Trust, Bristol, United Kingdom - Bucciarelli-Ducci C | University Hospital Brussels, Brussels, Belgium – Weytjens C | University Hospital of Geneva, Geneva, Switzerland – Tessitore E | University Hospitals of Leicester NHS Trust, Leicester, United Kingdom - McCann G | University Medical Center Groningen, Groningen, the Netherlands – van Gilst WH | University Medical Center Utrecht, Utrecht the Netherlands – Asselbergs FW, Linschoten M, van der Harst P | van Weel-Bethesda Hospital, Dirksland, the Netherlands – Wu KW | Zaans Medical Center, Zaandam, the Netherlands – DO | Hospital Group Twente, Almelo, the Netherlands - Linssen GCM | Zuyderland Medical Center, Heerlen, the Netherlands - Kietselaer BLJH.

References

- [1] Aghagoli G, Gallo Marin B, Soliman LB, et al. Cardiac involvement in COVID-19 patients: Risk factors, predictors, and complications: A review. *J Card Surg* 2020;35(6):1302-05. doi: 10.1111/jocs.14538
- [2] Puntmann VO, Carerj ML, Wieters I, et al. Outcomes of cardiovascular magnetic resonance imaging in patients recently recovered from coronavirus disease 2019 (COVID-19). *JAMA Cardiol* 2020 doi: 10.1001/jamacardio.2020.3557
- [3] Wagner P, Strodthoff N, Bousseljot RD, Kreiseler D, Lunze FI, Samek W and Schaeffter T. PTB-XL, a large publicly available electrocardiography dataset. *Sci Data*. 2020;7:154.
- [4] van Dam PM. A new anatomical view on the vector cardiogram: The mean temporal-spatial isochrones. *J Electrocardiol*. 2017;50:732-738.
- [5] van Dam PM, Locati ET, Ciconte G, Borrelli V, Heilbron F, Santinelli V, Vicedomini G, Monasky MM, Micaglio E, Giannelli L, Mecarocci V, Čalović Ž, Anastasia L and Pappone C. Novel CineECG derived from standard 12-Lead ECG enables right ventricle outflow tract localization of electrical substrate in patients with Brugada syndrome. *Circulation: Arrhythmia and Electrophysiology*. Published online 28 July 2020.

Address for correspondence.

Peter M van Dam

Weiland 38, 2415BC Nieuwerbrug aan den Rijn, the Netherlands

E-mail address: peter.van.dam@peacs.nl